Soft Matter

Viscoelastic multistable architected materials with temperature-dependent snapping sequence

Journal:	*Soft Matter*
Manuscript ID	SM-ART-01-2018-000217.R1
Article Type:	Paper
Date Submitted by the Author:	23-Feb-2018
Complete List of Authors:	Che, Kaikai; Georgia Institute of Technology, Woodruff Shool of Mechanical Engineering Yuan, Chao; Georgia Institute of Technology, School of Mechanical Engineering Qi, H.; Georgia Institute of Technology, School of Mechanical Engineering Meaud, Julien; Georgia Institute of Technology, Woodruff Shool of Mechanical Engineering

Viscoelastic multistable architected materials with temperature-dependent snapping sequence

Kaikai Che[1], Chao Yuan[1,2], Jerry H. Qi[1], and Julien Meaud [*1]

[1]*G.W.W. School of Mechanical Engineering, Georgia Institute of Technology, Atlanta USA*

[2]*State Key Laboratory for Strength and Vibration of Mechanical Structures,Department of Engineering Mechanics, School of Aerospace Engineering, Xi'an Jiaotong University, China*

February 23, 2018

[*]Corresponding author: julien.meaud@me.gatech.edu

Abstract

When an architected material with snap-through instabilities is loaded, the unit cells of the architected material snap sequentially to a series of deformed configurations. In this paper, we propose the novel concept of multimaterial viscoelastic architected materials whose snapping sequence can be tuned using temperature as a control parameter. Because different polymers have different temperature-dependent properties, it is possible that one polymer that is stiffer than another polymer at one temperature becomes softer at a higher temperature. A 3D printing inverse molding process is used to fabricate soft multimaterial architected materials that consist of two different polymers. Using finite element simulations and experiments, we demonstrate that the snapping sequence of these multimaterial architected materials depends on temperature. The influence of the geometrical parameters of the design on the critical temperature at which the snapping sequence switches from one sequence to another sequence is systematically analyzed using simulations and experiments. Being able to tune the snapping sequence using temperature makes it possible to obtain a large number of distinct stable configurations in response to compressive loads. To illustrate a potential application, we demonstrate that these materials can be used as soft reconfigurable metamaterials with tunable stiffness.

1 Introduction

Architected materials (also called mechanical metamaterials) are materials whose effective properties emerge from their periodic microarchitecture rather than from the intrinsic properties of their constituent materials [1, 2]. The functionality of architected materials can be enhanced by exploiting elastic instabilities that cause configurational changes in the architecture [3]. For example, pattern transformations induced by mechanical instabilities under compression can be used to design soft reconfigurable phononic crystals that can be reversibly tuned by applying a deformation [4, 5]; similar pattern transformations can be exploited to obtain color switching in polymeric membranes [6]. The development of smart materials that can be programmed on demand would be useful in a number of applications, such as soft robotics, shape morphing or biomedical devices [7].

This paper focuses on reconfigurable architected materials made of unit cells with snap-through instabilities. Snap-through buckling is a kind of elastic instability that causes a structure to jump from one configuration to another configuration when an applied stimulus reaches a critical level due to the non-convexity of the strain energy potential [8]. Depending on the strain energy curve of the system, a system with snap-through instability may be monostable (it returns to its initial undeformed configuration after the removal of the load) or bistable (it remains in a deformed state when the external load is released). Architected materials made up of multiple unit cells with snap-through instabilities in series have found interesting applications. For example, these types of architected materials have excellent energy dissipation capabilities in response to cyclic loadings due to the emergence of large hysteresis loops [9, 10]. Furthermore, multistable systems that consist of multiple bistable unit cells can absorb mechanical energy in response to impacts [11, 12], have interesting shape morphing properties [13] or let elastic wave propagate in soft media despite the presence of viscoelastic dissipation [14]. More recently, Meaud and Che [15] demonstrated that multistable architected materials can be used as reconfigurable phononic crystals with broadband phononic band gaps; switching from one stable configuration to another one allows to switch on/off

the propagation of elastic waves. One advantage of reconfigurable metamaterial made of bistable unit cells is that the system is able to remain in a deformed stable configuration after removal of the external stimulus.

However, being able to obtain in a deterministic manner a given stable configuration is essential for the application of these architected materials as reconfigurable metamaterials that can be programmed by applying an external stimulus. When a material made of unit cells with snap-through instabilities in series is progressively loaded, the unit cells snap sequentially [10, 16, 12]. If all unit cells are identical, the sequence of stable configurations (which we will call the snapping sequence in the remainder of the manuscript) is unpredictable due to the effect of imperfections in the geometry, material properties or boundary conditions. While a deterministic snapping sequence can be obtained by varying the unit cell's geometrical parameters [16, 12], the snapping sequence is predefined and cannot change after fabrication. In order to overcome this limitation and to enhance the tunability, we propose to develop multimaterial viscoelastic architected materials and to reversibly tune the snapping sequence using temperature as a control parameter. While it has been previously shown that viscoelastic effects can be exploited to tune the elastic instabilities of multimaterial structures and materials such as thin films on soft substrates [17, 18, 19] or layered composites [20, 21, 22], using these effects to tune the snapping response of architected materials with snap through instabilities is a novel idea.

The main objective of this paper is to investigate the temperature-dependent switching of the snapping sequence of multimaterial viscoelastic architected materials. The influence of temperature on the snapping sequence is analyzed using numerical simulations and experiments. To illustrate a potential application of these architected materials as soft reconfigurable materials with tunable stiffness, we also determine the effective stiffness of these architected materials in each of the stable configurations that are obtained in response to compressive deformations.

2 Methods

2.1 Design of architected materials with bistable unit cells

As in our previous work [16], the proposed architected materials consist of N layers (in series) of unit cells with snap-through instabilities (Fig. 1). Because of the thin curved part of the unit cell of thickness t and initial apex height h, the unit cells have a negative stiffness once the applied force reaches a critical value (Fig. 1C); under force control, the unit cell snaps through. Two non-dimensional parameters, $Q = h/t$ and $P = l/t$, have the main influence on the mechanics of the unit cell. As shown in Fig. 1C, the value of Q primarily determines whether the unit is monostable or bistable, while the value of P influences the stiffness of the unit cell. For example, the unit cell is bistable for $Q = 3$ and $P = 13.65$ since there are two points of zero force and positive slope in the force vs deflection curve; when Q is reduced to 2.8, the unit cell is monostable since the force is always $\neq 0$ except for the initial undeformed configuration; for $Q = 3$ and $P = 15.17$, the unit cell is bistable but its stiffness in the stable deformed configuration is lower stiffness than when $Q = 3$ and $P = 13.65$.

In contrast to our previous work, the different layers of the architected material are made of different materials. For example, for the architected material shown in Figs. 1D, the top two layers are made of PEGDA while the other layers are made of a 3D printed polymer, DM8995 (a digital material made of the mixture of two base materials; we will refer to DM8995 as DM hereafter).

A.

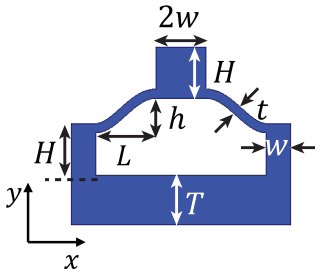

B.

Geometrical parameter	Value
t	$t_0 \sim 2t_0$
h	Qt
L	Pt
T	$11.6t_0$
H	$6t_0$
w	$5.8t_0$

C.

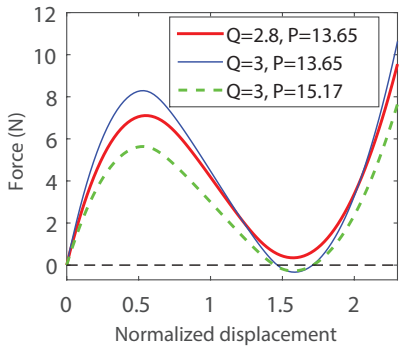

D.

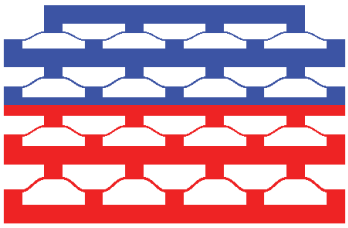

Figure 1: Bi-material architected materials with snap-through instabilities. A. Unit cell . B. Values of unit cell's geometrical parameters. Q and P are non-dimensional parameters that are varied in the manuscript. Fabricated samples use $t_0 = 0.25$mm and an out-of-plane thickness of 6mm. C. Influence of P and Q on the force vs normalized deflection ($\bar{d} = d/h$ where d is the displacement of the top edge of the unit cell) curve for a single elastic unit cell. D. Example of 4-layer architected material (N=4). The blue color corresponds to PEGDA and the red color to DM.

2.2 Fabrication of multimaterial architected materials using an inverse molding process

3D printing is a powerful fabrication tool to create structures with complicated geometries. However, a very limited number of materials can be 3D printed, which limits the applications of 3D printing to multimaterial reconfigurable architected materials. While the polyjet-based method allows three or more materials to be printed simutaneously, the number of available materials in the

polyjet based method is extremely limited (for example less than 10 polymers for the newest 3D printer models of the Stratasys Objet Connex series polyjet 3D printers). To have more freedom in the material choice, we implemented a facile 3D printing inverse molding process (Fig. 2A). We first printed a periodic structure using a 3D printer (Objet Connex 260, Stratasys, Edina, MN, USA) made of a 3D printed material (DM), which served as a positive mold to make a PDMS mold (end of Step 1). The PDMS mold was then used to replicate the periodic structure, but with different materials. In the example shown in Fig. 2, we first fill half of the mold with a 3D printed half structure printed using DM; we then fill the rest of the space by a photocurable Poly(ethylene glycol) diacrylate (PEGDA) resin. After curing, we obtain a bi-material architected material (Fig. 2B). The advantage of this approach is that it removes the material choice constraints imposed by 3D printing. For example, we were able to select PEGDA, whose dependence of storage modulus on the temperature crosses that of 3D printed materials (see Fig. 3A); such a crossover renders very exciting behaviors, which could not be achieved if one solely relies on the 3D printed materials.

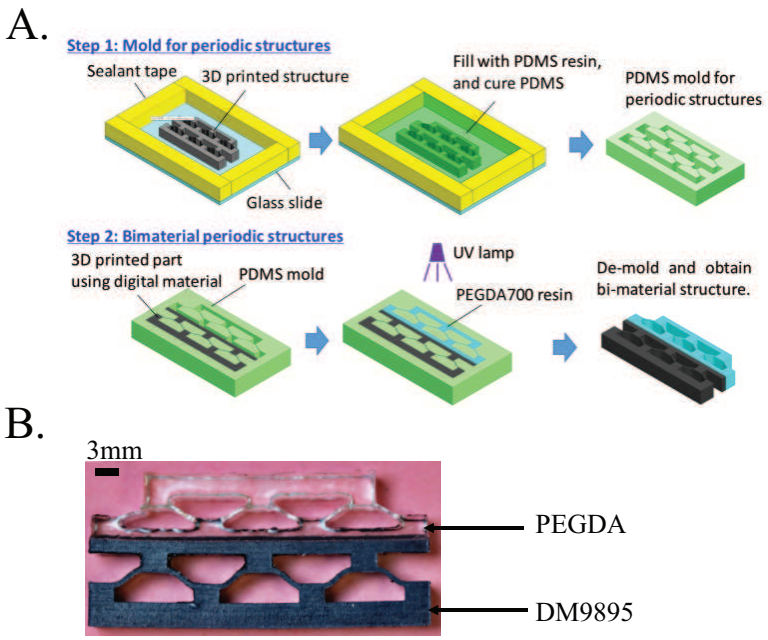

Figure 2: A. Fabrication process for multimaterial architected materials. B. Example of fabricated bi-material sample.

2.3 Mechanical testing

The samples were compressed at a constant velocity $v = 10$mm/min using a universal Material Testing System (MTS, Model Insight 10, Eden Prairie, MN, USA) in a displacement control manner with a 10kN load cell. The experiments were conducted in a temperature controlled box. For experiments that were conducted at temperature above room temperature, the temperature was first increased, then held for 10 min (such that the temperature of the sample reaches its steady-state value) before doing the compression test.

2.4 Finite element models

Besides compression experiments, the mechanics of these multistable architected materials were analyzed using two-dimensional finite element models. 4-node bilinear quadrilateral plane-stress

elements with reduced integration (CPS4R in Abaqus) were used. Self-contact normal interactions were defined for the whole model. The response of the architected material was simulated using a quasi-static step (VISCO step in ABAQUS/Standard) with nonlinear geometry. Because the modulus of PEDGA is almost temperature-indendent in the temperature range that was considered (see Fig. 3A), PEDGA was modeled as an isotropic, elastic constitutive material. An isotropic, thermo-viscoelastic constitutive model was used for DM since its modulus is temperature-independent (see Fig. 3A). For this thermo-viscoelastic model, the temperature-dependent relaxation modulus, $E(t,T)$, is expressed as a Prony series of the form:

$$E(t,T) = E_{eq} + \sum_{i=1}^{n} E_i \exp\Big[-\frac{t}{\tau_i(T)}\Big] \tag{1}$$

where t is the time, T is the temperature, E_{eq} is the Young's modulus of the equilibrium branch, n is the number of viscoelastic branches, E_i (where $i-1,..,n$) is the Young's modulus of the viscoelastic branches, and τ_i is relaxation time, which is expressed as,

$$\tau_i(T) = \alpha(T)\tau_i^0 \tag{2}$$

where τ_i^0 is a constant and $\alpha(T)$ is a temperature-dependent shifting factor. Above the reference temperature, $\alpha(T)$ is given by the Williams-Landel-Ferry (WLF) equation [23, 24]:

$$\log\Big[\alpha(T)\Big] = -\frac{C_1(T-T_M)}{C_2+(T-T_M)} \tag{3}$$

where C_1 and C_2 are material constants and T_M is the WLF reference temperature. The value of the material parameters are given in the Supporting Information.

3 Results and discussions

3.1 The snapping sequence can be tuned using temperature

Bilayer samples (Fig. 3B) made of PEDGA and DM were fabricated using the inverse molding process described in the Methods section. The two materials, PEDGA and DM, were chosen

because their storage moduli cross over at a temperature near room temperature, at about 32^oC (Fig. 3A). This cross-over in the stiffness of the two layers is the physical basis for the temperature-dependent switch in the snapping sequence. The bilayer samples were compressed by moving a loading cell at a constant velocity. When a bilayer sample is compressed, the layer with the lower stiffness snaps before the other layer snaps. Hence, due to the temperature-dependent modulus of DM, the snapping sequence (which layer snaps first and second) can be tuned by temperature: at room temperature (T=20^oC), DM is much stiffer than PEDGA (Fig. 3A), therefore, the top layer (L2) snaps first (as seen in Fig. 3C); however, the snapping sequence changes when the compression test is conducted at 50^oC, where DM is softer than PEGDA (Fig. 3A) and the bottom layer (L1) snaps first (as seen in Fig. 3E). To more quantitatively evaluate the snapping sequence, the deformation of the bottom layer, $d_1(\varepsilon)$, and top layer, $d_2(\varepsilon)$, were calculated using:

$$\begin{aligned} d_1(\varepsilon) &= u_1(\varepsilon) \\ d_2(\epsilon) &= u_2(\varepsilon) - u_1(\varepsilon) \end{aligned} \tag{4}$$

where $u_1(\varepsilon)$ and $u_2(\varepsilon)$ are the displacements of bottom layer and top layer, respectively (shown in Fig. 3B) and ε is the effective strain (computed using $\varepsilon = u_2/h_{tot}$ where h_{tot} is the total height of the sample). At low temperature, it is observed that the value of d_2 rises before the value of d_1, while the opposite trend is observed at high temperature. While the snapping of each layer would be instantaneous if elastic materials would be used, the snapping of each layer is more gradual here due to the presence of viscoelasticity. The finite element simulations agree very well with the experiments both at the low (Fig. 3D) and high (Fig. 3F) temperatures.

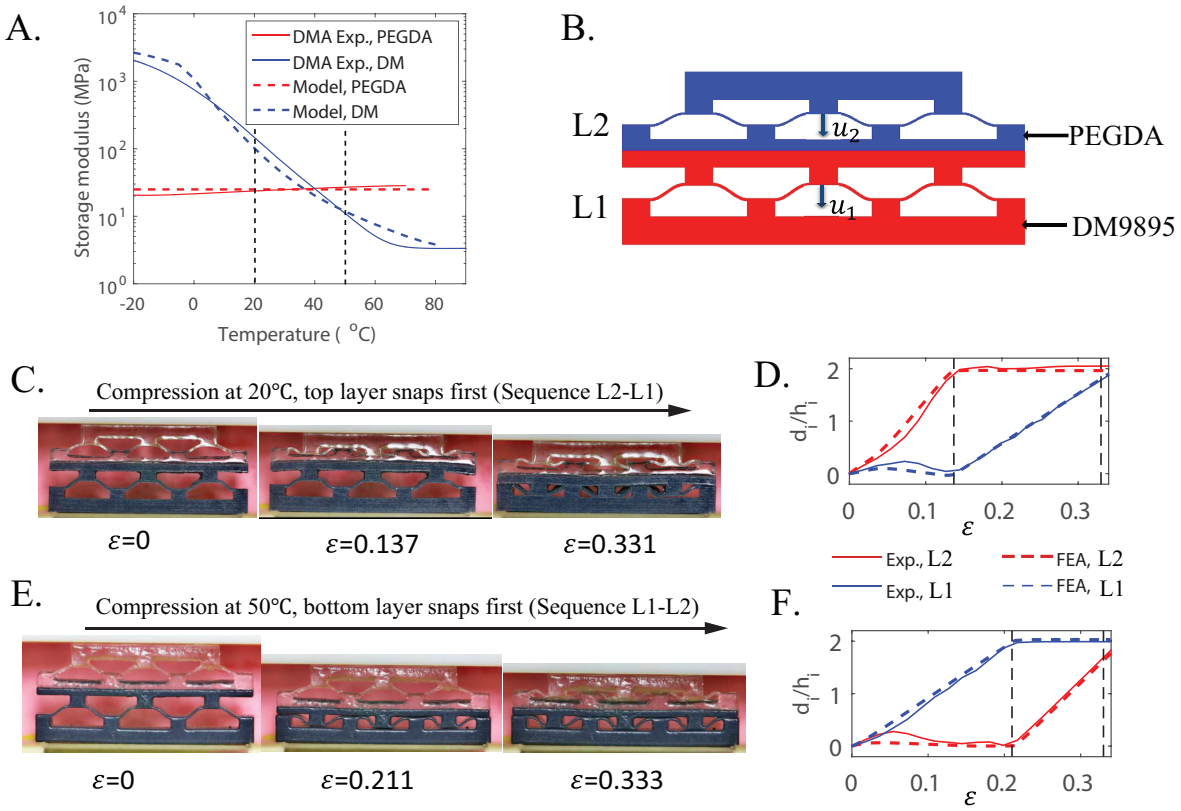

Figure 3: Tuning the snapping sequence using temperature. A. Storage modulus vs temperature for PEDGA and DM at 1Hz. B. Schematics of bilayer sample. u_1 and u_2 are the displacements of the bottom and top layers, respectively. C. and E. Snapshots of the compression tests at 20^oC and 50^oC. D. and F. Comparison of the normalized deformation for the bottom layer, d_1/h_1, and top layer, d_2/h_2, as a function of the effective strain, ϵ, at 20^oC (D) and 50^oC (F). The vertical dashed lines corresponds to the effective strain value in the snapshots of panels C and E.

3.2 Influence of the geometrical parameters on the critical temperature

Because of the high fidelity of the finite element simulations, the influence of the geometrical parameters on the snapping sequence was systematically studied using numerical results. The tem-

perature at which the snapping sequence switches from the sequence observed at room temperature (*i.e.*, the PEDGA layer snaps first) to the sequence observed at high temperature (*i.e.*, the DM layer snaps first) was defined to be the critical temperature, T_{cr}. The thickness of the curved part of the unit cell, t (see Fig. 1B), significantly influences the stiffness of the unit cell. Hence, we analyzed the influence on T_{cr} of the ratio of the t value for the DM layer, t_1, to the t value for the PEDGA layer, t_2. For these simulations, t_2 was kept constant while t_1 was varied between t_2 and 1.65 $\times t_2$ (while keeping the non-dimensional parameter $Q_2 = h_2/t_2$ constant).

The numerical results shown in Fig. 4 demonstrate that the critical temperature increases when t_1/t_2 increases. This is due to the increase in the stiffness of the DM layer relative to the stiffness of the PEDGA layer. When the thickness ratio is high enough ($t_1/t_2 \geq 1.65$), no switching of the snapping sequence is observed: at all temperatures, the top layer (PEDGA) snaps first. This can explained by the fact that the modulus of DM saturates to a constant value at high temperature (Fig. 3A). For validation of these numerical results, the transition temperature was also determined experimentally for 22 different samples fabricated using the inverse mold fabrication method. For each sample, tests were repeated at multiple temperatures in order to determine with a 1 degree accuracy the value of the critical temperature. The critical temperatures obtained experimentally follow closely the trend observed in the finite element simulations; furthermore, as in the simulations, no switch was observed when $t_1/t_2 \geq 1.65$.

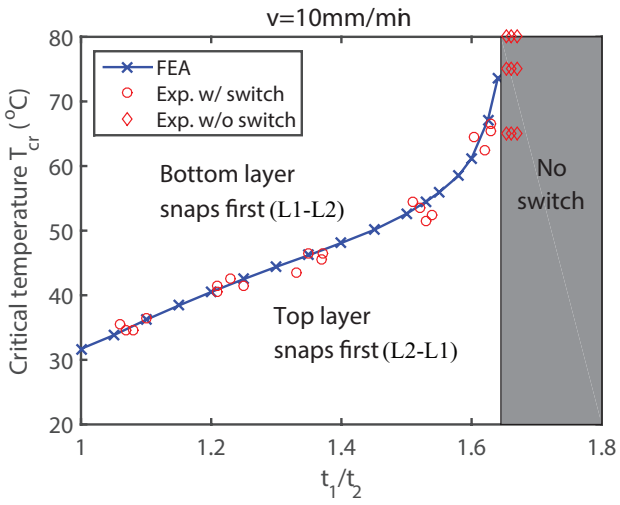

Figure 4: Critical temperature vs thickness ratio. The red circles correspond to the values of T_{cr} determined using compression test with fabricated samples. The red diamonds correspond to tested temperatures for samples for which no switch was observed.

3.3 Multiple snapping sequence switchings in N-layer architected materials

The ability to tune the value of T_{cr} by varying the geometrical parameters of the layers can be exploited to considerably expand the number of stable configurations that can be obtained in response to a compressive deformation for architected materials that consist of $N > 2$ layers. A multistable architected material with N layers of bistable unit cells in series has a total of $N_{tot} = 2^N$ stable configurations. These stable configurations can be identified by a combination of binary numbers $i_1, ..., i_N$, where i_j (j=1,...,N) corresponds to the stable configuration of layer j (where $i_j = 0$ and $i_j = 1$ correspond to the undeformed and stable configurations, respectively). However, only a small portion of these stable configurations can be obtained by a applying a compressive deformation if temperature-dependent viscoelastic effects are not exploited: the number of stable configurations obtained as a single temperature using a compressive deformation is only $N_{single} = N + 1$. For example consider the 4-layer sample shown in Fig. 5A that consists of two DM layers (lay-

ers 1 and 2) and two PEGDA layers (layers 3 and 4). The two DM layers have different t values ($t_1 > t_2$) and the two PEDGA layers have different t values ($t_3 > t_4$). At room temperature, only the configurations 0000, 0001, 0111, 0111 and 1111 can be obtained in response to a compressive deformation (Fig. 5C). However, because of the variations in the t values, four different critical temperatures can be identified: between layers 1 and 3, between layers 1 and 4, between layers 2 and 3 and between layers 2 and 4. Hence, this makes it possible to obtain $N_{seq} = 5$ different snapping sequences, depending on the temperature (Fig. 5C), which results in a total of nine different configurations (shown in the last column of Fig. 5C) that can be obtained in response to a compressive deformation.

More generally, as shown in the Supporting Information, the maximum number of different snapping sequences that can be obtained by exploiting temperature-dependent viscoelastic effects for a bi-material architected material with N layers is:

$$N_{seq,max}(N) = \lfloor \frac{N}{2} \rfloor \lfloor \frac{N+1}{2} \rfloor + 1 \tag{5}$$

where $\lfloor . \rfloor$ denotes the floor function. The total number of different stable configurations that are obtained in response to compressive loads at multiple temperatures is:

$$N_{bimat}(N) = \lfloor \frac{N}{2} \rfloor \lfloor \frac{N+1}{2} \rfloor + N + 1 \tag{6}$$

As shown in Fig. 5B, N_{bimat} is significantly larger than N_{single} for large N values. Temperature-dependent viscoelastic effects make it possible to considerably expand the number of stable configurations that can be obtained in response to compressive loads.

A.

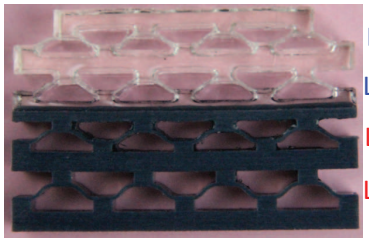

B.

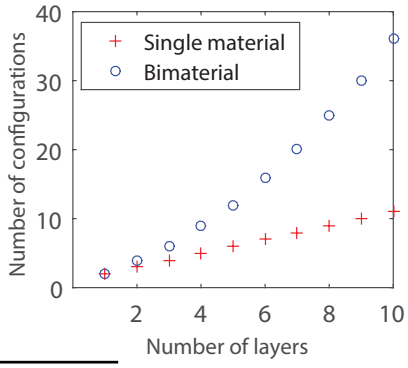

C.

Temperature (°C)	Snapping sequence	Configurations
$T < 31$	L4-L3-L2-L1	0000, 0001, 0011, 0111, 1111
$31 < T < 41$	L4-L2-L3-L1	0000, 0001, 0101, 0111, 1111
$41 < T < 46$	L2-L4-L3-L1	0000, 0100, 0101, 0111, 1111
$46 < T < 62$	L2-L4-L1-L3	0000, 0100, 0101, 1101, 1111
$T > 62$	L2-L1-L4-L3	0000, 0100, 1100, 1101, 1111

Figure 5: Stable configurations and snapping sequences for N-layer bi-material architected materials. A. Example of 4-layer bi-material architected material where $t_2 = t_3 = 1.2t_4$ and $t_1 = 1.6t_4$. B. Snapping sequences and configurations at different temperatures. C. Number of stable configurations obtained in response to compressive deformation as function of the number of layers.

3.4 Exploiting temperature-dependent snapping sequences to obtain materials with tunable stiffness

The ability of these architected materials to have multiple stable configurations can be exploited to obtain reconfigurable materials with tunable stiffness. Because these architected materials consist of N layers in series, they can be modeled as 1D chains of nonlinear springs. The effective dynamic stiffness of the architected material in response to cyclic loads in configuration $i_1, ..., i_N$ can be

estimated using the equation:

$$k^*_{eff,i_1,\ldots,i_N}(\omega,T) = \Big[\sum_{j=1}^{N} \frac{1}{E^*_j(\omega,T)k_{j,i_j}}\Big]^{-1} \tag{7}$$

where k_{j,i_j} is the normalized stiffness of layer j in configuration i_j and E^*_j is the dynamic Young's modulus of the material used for layer j; and * denotes a complex number. k_{j,i_j} was computed using the analysis of a single elastic layer (described in the Supporting Information) using the following definition:

$$k_{j,i_j} = \frac{1}{E}\frac{dF}{du}(u_{i_j}) \tag{8}$$

where E is the Young's modulus, F is the applied force, u is the deflection of the layer and u_{i_j} is the deflection of the layer in configuration i_j.

We analyzed the stiffness of all the stable configurations that can be obtained by exploiting temperature-dependent viscoelasticity in bimaterial architected materials made of 4 layers. For the design previously shown in Fig. 5A, the variations in the stiffnesses of these nine stable configurations is relatively limited (Fig. 6C): for example, the fully deformed configuration is only 39% softer than the undeformed configuration; the difference between the stiffnesses in Configurations 0111 and 1111 is only 2% of the stiffness in Configuration 0000. To obtain a design with highly tunable stiffness values, we considered a wide range of values for the non-dimensional parameters $Q_j = h_j/t_j$ and $P_j = l_j/t_j$ of each layer, as shown in the Supporting Information. To find a set of parameters such that the stiffnesses of each of the stable configurations are significantly different, we chose the design that maximizes the following objective function:

$$f(Q_1,Q_2,Q_3,Q_4,P_1,P_2,P_3,P_4) = \min_{i_1i_2i_3i_4 \neq j_1j_2j_3j_4} \frac{|k_{eff,i_1i_2i_3i_4} - k_{eff,j_1j_2j_3j_4}|}{k_{eff,0000}} \tag{9}$$

where $i_1i_2i_3i_4$ and $j_1j_2j_3j_4$ corresponds to different stable configurations; k_{eff}, is the real part of the dynamic stiffness computed using Eq. 7. As seen in Fig. 6B, the nine stable configurations of the best design have stiffness values (all calculated at room temperature using Eq. 7) that vary more significantly than in the initial design: for example, Configuration 1111 is 66% softer

than Configuration 0000; the difference in the stiffness values of the two configurations that have the most similar stiffness (Configurations 0111 and Configuration 1111) is 4% of the stiffness in Configuration 0000.

To confirm that this architected material exhibits significant deformation-induced tunability of its stiffness, the stiffness of these nine configurations was also directly calculated using finite element simulations of the 4-layer architected material. For these simulations, the material was first loaded at room temperature in the cases of Configurations 0001, 0011, 0111 and 1111. In order to compute the effective stiffness in other configurations, the architected material was first loaded at a higher temperature until the corresponding layers snap, before changing the temperature to room temperature. For all nine configurations, the effective dynamic stiffness was computed by applying a harmonic velocity of small amplitude at room temperature. While small quantitative differences with the spring model are observed, the stiffness obtained with these direct FEA simulations also show that the nine stable configurations have significantly different effective stiffnesses (Fig. 5B);

Examination of the parameters for the best design (Fig. 6D and Fig. S1 in the Supporting Information) makes it possible to get some insight about what is required to obtain highly tunable stiffness. The parameters of three of the four layers are close to the limit between monostable and bistable behaviors. When the geometrical parameters of a single layer of unit cells are such that the unit cells are close to the limit between monostable and bistable behaviors, the stiffness in the undeformed configuration is much higher than the stiffness in the deformed configuration, as shown in our recent work [15]. Because of the significant difference between the stiffness in the undeformed and deformed configurations of each unit cell, snapping from one configuration to another configuration causes a significant change in the effective stiffness of the architected material.

Other researchers have used temperature-induced effects to develop programmable materials with tunable stiffness. For example, Restrepo *et al.* [25, 26] recently proposed periodic cellular solids with tunable stiffness by introducing controlled morphological imperfections into the unit

cells and exploiting the shape memory effect. Haghanah et al. [13] introduced programmable metamaterials that can be tuned using via actuation of embedded electromagnetic locks. In contrast to our work which is limited to architected materials that only have tunable properties in the vertical (y) direction, these materials are truly two-dimensional materials. However, a key advantage of our approach is that is possible to use a simple model based on a 1D chain of elastic springs to predict with great accuracy the stiffness of an architected material with N layers. This spring model facilitates the design of materials with prescribed tunable stiffness properties.

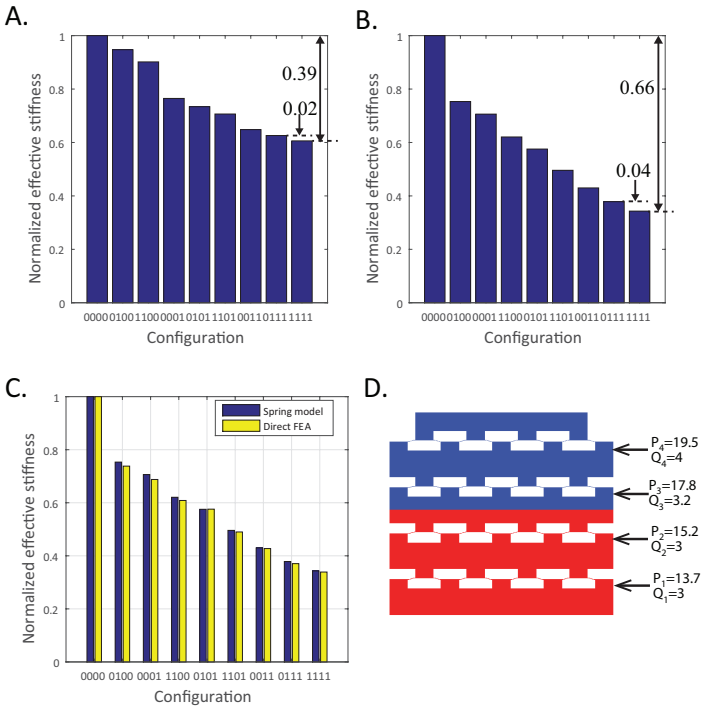

Figure 6: Normalized effective stiffness of the stable configurations for 4-layer architected materials. A. and B. Stiffness values obtained with the spring model for the design of Fig. 5 (A) and the best design (B). C. Comparison of the stiffness values obtained with the spring model and the direct finite element simulations for the best design. The stiffness values are normalized to the stiffness value in the undeformed configuration (Configuration 0000). D. Schematics and parameter values for the best design.

4 Conclusions

These numerical and experimental results demonstrate that the snapping sequence of multimaterial viscoelastic architected materials can be tuned by varying the ambient temperature. In contrast to architected materials that consist of a single material [16, 12], temperature can be used as a control parameter to tune the behavior of these smart materials after fabrication. This novel physical

behavior is made possible by the use of viscoelastic materials whose moduli cross-over close to room temperature. The temperature-dependent switching of the snapping sequence of bilayer bimaterial architected material was systematically investigated using finite element simulations and experiments with samples fabricated using an inverse molding process. The influence of the geometrical parameters on the critical temperature at which the snapping sequence switches from one sequence to another sequence was analyzed. The reversible configurational changes in these architected materials can be exploited to develop materials that are reconfigurable based on the desired functionality. Exploiting the temperature-dependent snapping sequence in bimaterial architected materials that consist of a large number of unit cells makes it possible to obtain a large number of distinct stable configurations only by applying a compressive load at different temperatures. With a proper choice of design parameters, each of these distinct stable configurations can have a unique value in its effective properties; we demonstrated that these materials can be for example as programmable soft materials with tunable stiffness.

5 Acknowledgments

This research was supported in part by NSF Award No. CMMI-1462894 to H. Jerry Qi.

References

[1] Tobias A Schaedler and William B Carter. Architected cellular materials. *Annual Review of Materials Research*, 46:187–210, 2016.

[2] Amir A Zadpoor. Mechanical meta-materials. *Materials Horizons*, 3(5):371–381, 2016.

[3] Nan Hu et al. Buckling-induced smart applications: recent advances and trends. *Smart Materials and Structures*, 24(6):063001, 2015.

[4] K Bertoldi, MC Boyce, S Deschanel, SM Prange, and T Mullin. Mechanics of deformation-triggered pattern transformations and superelastic behavior in periodic elastomeric structures. *Journal of the Mechanics and Physics of Solids*, 56(8):2642–2668, 2008.

[5] Jongmin Shim, Pai Wang, and Katia Bertoldi. Harnessing instability-induced pattern transformation to design tunable phononic crystals. *International Journal of Solids and Structures*, 58:52–61, 2015.

[6] Jie Li, Jongmin Shim, Justin Deng, Johannes TB Overvelde, Xuelian Zhu, Katia Bertoldi, and Shu Yang. Switching periodic membranes via pattern transformation and shape memory effect. *Soft Matter*, 8(40):10322–10328, 2012.

[7] Pedro M Reis, Heinrich M Jaeger, and Martin van Hecke. Designer matter: A perspective. *Extreme Mechanics Letters*, 5:25–29, 2015.

[8] George J Simitses and Dewey H Hodges. *Fundamentals of structural stability*. Butterworth-Heinemann, 2006.

[9] Dixon M Correa, Timothy Klatt, Sergio Cortes, Michael Haberman, Desiderio Kovar, and Carolyn Seepersad. Negative stiffness honeycombs for recoverable shock isolation. *Rapid Prototyping Journal*, 21(2):193–200, 2015.

[10] David Restrepo, Nilesh D Mankame, and Pablo D Zavattieri. Phase transforming cellular materials. *Extreme Mechanics Letters*, 4:52–60, 2015.

[11] Sicong Shan, Sung H Kang, Jordan R Raney, Pai Wang, Lichen Fang, Francisco Candido, Jennifer A Lewis, and Katia Bertoldi. Multistable architected materials for trapping elastic strain energy. *Advanced Materials*, 27(29):4296–4301, 2015.

[12] Tobias Frenzel, Claudio Findeisen, Muamer Kadic, Peter Gumbsch, and Martin Wegener. Tailored buckling microlattices as reusable light-weight shock absorbers. *Advanced Materials*, 2016.

[13] Babak Haghpanah, Ladan Salari-Sharif, Peyman Pourrajab, Jonathan Hopkins, and Lorenzo Valdevit. Multistable shape-reconfigurable architected materials. *Advanced Materials*, 28(36):7915–7920, 2016.

[14] Jordan R Raney, Neel Nadkarni, Chiara Daraio, Dennis M Kochmann, Jennifer A Lewis, and Katia Bertoldi. Stable propagation of mechanical signals in soft media using stored elastic energy. *Proceedings of the National Academy of Sciences*, page 201604838, 2016.

[15] Julien Meaud and Kaikai Che. Tuning elastic wave propagation in multistable architected materials. *International Journal of Solids and Structures*, 2017.

[16] Kaikai Che, Chao Yuan, Jiangtao Wu, H Jerry Qi, and Julien Meaud. Three-dimensional-printed multistable mechanical metamaterials with a deterministic deformation sequence. *Journal of Applied Mechanics*, 84(1):011004, 2017.

[17] R Huang and Z Suo. Instability of a compressed elastic film on a viscous layer. *International Journal of Solids and Structures*, 39(7):1791–1802, 2002.

[18] R Huang and Z Suo. Wrinkling of a compressed elastic film on a viscous layer. *Journal of Applied Physics*, 91(3):1135–1142, 2002.

[19] Sourav Chatterjee, Christina McDonald, Jiani Niu, Sachin S Velankar, Peng Wang, and Rui Huang. Wrinkling and folding of thin films by viscous stress. *Soft Matter*, 2015.

[20] Kashyap Alur and Julien Meaud. Nonlinear mechanics of non-dilute viscoelastic layered composites. *International Journal of Solids and Structures*, 72:130–143, 2015.

[21] Kashyap Alur, Thomas Bowling, and Julien Meaud. Finite-element analysis of rate-dependent buckling and postbuckling of viscoelastic-layered composites. *Journal of Applied Mechanics*, 83(3):031005, 2016.

[22] Viacheslav Slesarenko and Stephan Rudykh. Harnessing viscoelasticity and instabilities for tuning wavy patterns in soft layered composites. *Soft matter*, 12(16):3677–3682, 2016.

[23] Malcolm L Williams, Robert F Landel, and John D Ferry. The temperature dependence of relaxation mechanisms in amorphous polymers and other glass-forming liquids. *Journal of the American Chemical society*, 77(14):3701–3707, 1955.

[24] Kai Yu, Qi Ge, and H Jerry Qi. Reduced time as a unified parameter determining fixity and free recovery of shape memory polymers. *Nature communications*, 5:3066, 2014.

[25] David Restrepo, Nilesh D Mankame, and Pablo D Zavattieri. Programmable materials based on periodic cellular solids. part i: Experiments. *International Journal of Solids and Structures*, 100:485–504, 2016.

[26] David Restrepo, Nilesh D Mankame, and Pablo D Zavattieri. Programmable materials based on periodic cellular solids. part ii: Numerical analysis. *International Journal of Solids and Structures*, 100:505–522, 2016.

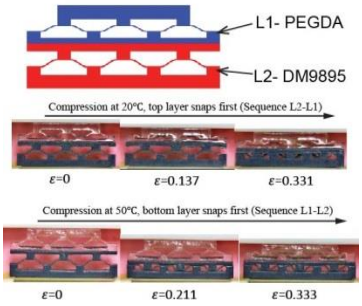

Novel concept of multimaterial architected materials whose snapping response can be controlled by varying the ambient temperature.